

Electronic Supplementary Information

Synthesis and Electrochemical properties of metal(II)-carboxyethylphenylphosphinates

Montse Bazaga-García,^a Álvaro Vílchez-Cózar,^a Bianca Maranescu,^b P. Olivera-Pastor,^a Marko Marganovici,^c Gheorghe Ilia,^{b,c} Aurelio Cabeza Díaz,^a Aurelia Visa^{*b} and Rosario M. P. Colodrero^{*a}

^aDpto Química Inorgánica, Cristalografía y Mineralogía, Facultad de Ciencias, Universidad de Málaga, Campus de Teatinos s/n, 29071-Málaga, Spain

^b"Coriolan Dragulescu" Institute of Chemistry, 24 Mihai Viteazu Blvd. 300223-Timisoara, Romania

^cWest University Timisoara, Faculty of Chemistry, Biology, Geography, Dept. of Biology-Chemistry, 16 Pestalozzi Street, 300115, Timisoara, Romania

Table of contents:

Figures:

Fig. S1 Final Rietveld plot for $\text{Cd}[\text{O}_2\text{P}(\text{CH}_2\text{CH}_2\text{COOH})(\text{C}_6\text{H}_5)]_2$ (**1**).

Fig. S2 Final Rietveld plot for $\text{Ca}[\text{O}_2\text{P}(\text{CH}_2\text{CH}_2\text{COOH})(\text{C}_6\text{H}_5)]_2$ (**2**).

Fig. S3 Final Rietveld plot for $\text{Co}_2[(\text{O}_2\text{P}(\text{CH}_2\text{CH}_2\text{COO})(\text{C}_6\text{H}_5)(\text{H}_2\text{O})]_2 \cdot 2\text{H}_2\text{O}$ (**3**).

Fig. S4 FT-IR spectra of: (a) $\text{Co}_3(\text{O}_2\text{P}(\text{CH}_2\text{CH}_2\text{COO})(\text{C}_6\text{H}_5)_2(\text{OH})_2$ (**4**), (b) $\text{Co}_2[(\text{O}_2\text{P}(\text{CH}_2\text{CH}_2\text{COO})(\text{C}_6\text{H}_5)(\text{H}_2\text{O})]_2 \cdot 2\text{H}_2\text{O}$ (**3**) and (c) $\text{Ca}[\text{O}_2\text{P}(\text{CH}_2\text{CH}_2\text{COOH})(\text{C}_6\text{H}_5)]_2$ (**2**).

Fig. S5 (a) Layered packing of $\text{Cd}[\text{O}_2\text{P}(\text{CH}_2\text{CH}_2\text{COOH})(\text{C}_6\text{H}_5)]_2$ (**1**) and (b) details of a hybrid layer in $\text{Cd}[\text{O}_2\text{P}(\text{CH}_2\text{CH}_2\text{COOH})(\text{C}_6\text{H}_5)]_2$ (**1**) showing the 8-member rings (A) and 14-member rings (B).

Fig. S6 Plots of the complex impedance plane for (a) CEPPA ligand and (b) $\text{Co}_2[(\text{O}_2\text{P}(\text{CH}_2\text{CH}_2\text{COO})(\text{C}_6\text{H}_5)(\text{H}_2\text{O})]_2 \cdot 2\text{H}_2\text{O}$ (**3**) at 95 %RH and various temperatures: 80 (black), 70 (red), 60 (green), 50 (blue), 40 (cyan), 30 (magenta) and 25 °C (yellow).

Fig. S7 Arrhenius plots for $\text{Co}_2[(\text{O}_2\text{P}(\text{CH}_2\text{CH}_2\text{COO})(\text{C}_6\text{H}_5)(\text{H}_2\text{O})]_2 \cdot 2\text{H}_2\text{O}$ (**3**) (red) and CEPPA ligand (blue) at 95 % RH and different temperatures.

Fig. S8 Comparative of XRPD patterns for (a) CEPPA ligand, and (b) $\text{Co}_2[(\text{O}_2\text{P}(\text{CH}_2\text{CH}_2\text{COO})(\text{C}_6\text{H}_5)(\text{H}_2\text{O})]_2 \cdot 2\text{H}_2\text{O}$ (**3**) samples, simulated XRPD (black) and as synthesized compound before (blue) and after (red) proton conductivity measurements and (c) XRPD patterns for **3**: as synthesized (black), anhydrous at 200 °C (blue) and rehydrated at 95% RH (red).

Fig. S9 PXRD patterns of the $\text{Co}_2[(\text{O}_2\text{P}(\text{CH}_2\text{CH}_2\text{COO})(\text{C}_6\text{H}_5)(\text{H}_2\text{O})]_2 \cdot 2\text{H}_2\text{O}$ (**3**) pyrolyzed at different temperatures and atmospheres.

Fig. S10 PXRD patterns of the $\text{Co}_3(\text{O}_2\text{P}(\text{CH}_2\text{CH}_2\text{COO})(\text{C}_6\text{H}_5)_2(\text{OH})_2$ (**4**) pyrolyzed at different temperatures and atmospheres.

Fig. S11 Nyquist plots for selected cobalt(II) phosphinates and selected calcinated derivatives.

Fig. S12 LSV curves of cobalt(II) phosphinates and their pyrolytic derivatives for the oxygen reduction reaction (ORR).

Fig. S13 PXRD pattern of **3@1000C_N₂** after OER test.

Fig. S14 XPS for Co 2p_{3/2} region of pyrolyzed derivatives of compound **3**, before (black line) and after OER (red line) and ORR (blue line) tests.

Tables:

Table S1. Selected bond lengths (Å) for compounds **1 – 3**.

Table S2. H-bond distances for $\text{Co}_2[(\text{O}_2\text{P}(\text{CH}_2\text{CH}_2\text{COO})(\text{C}_6\text{H}_5)(\text{H}_2\text{O})]_2 \cdot 2\text{H}_2\text{O}$ (**3**).

Table S3. XPS data for compound **3** and its pyrolyzed derivatives before and after OER and ORR tests.

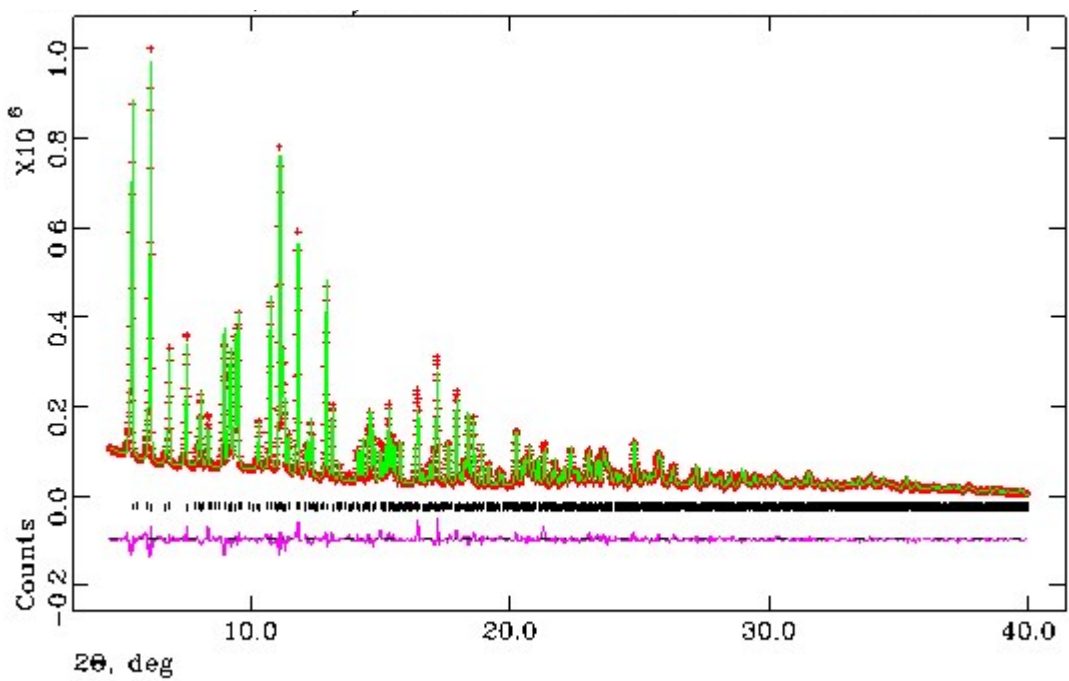


Fig. S1 Final Rietveld plot for **Cd[O₂P(CH₂CH₂COOH)(C₆H₅)₂] (1).**

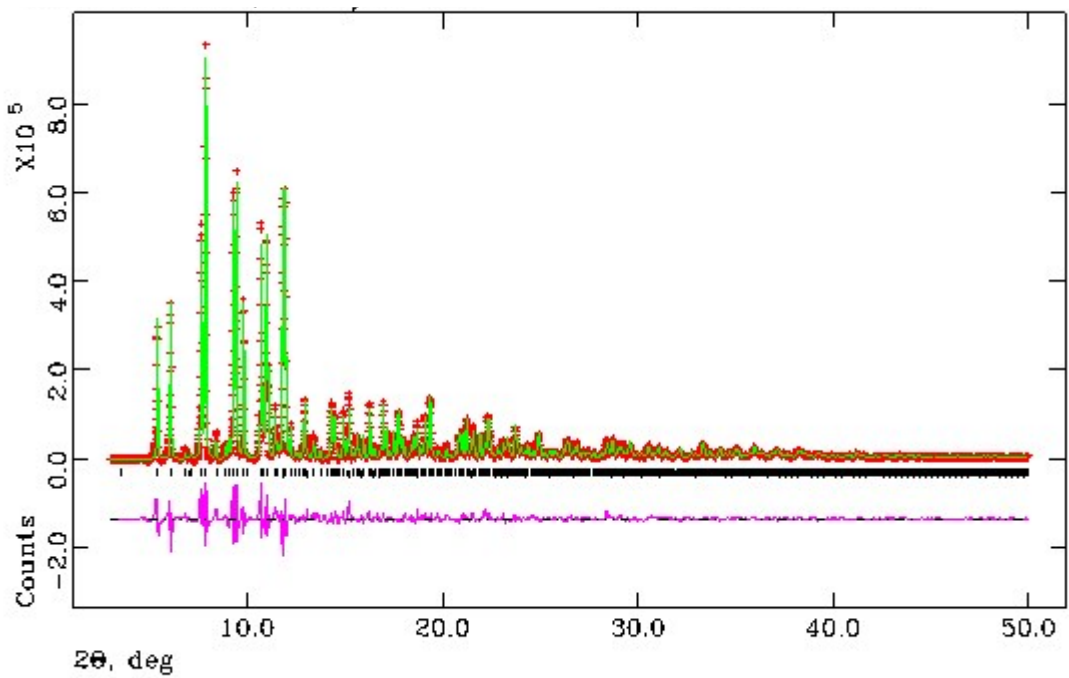


Fig. S2 Final Rietveld plot for **Ca[O₂P(CH₂CH₂COOH)(C₆H₅)₂] (2).**

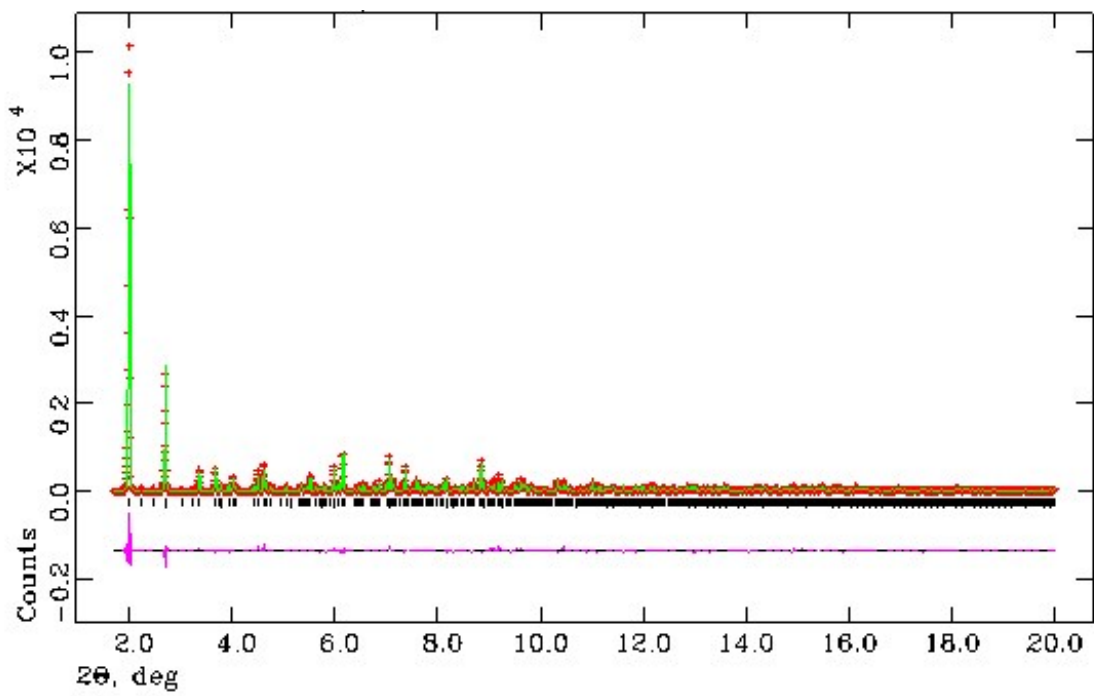


Fig. S3 Final Rietveld plot for $\text{Co}_2[(\text{O}_2\text{P}(\text{CH}_2\text{CH}_2\text{COO})(\text{C}_6\text{H}_5)(\text{H}_2\text{O}))_2 \cdot 2\text{H}_2\text{O}$ (3).

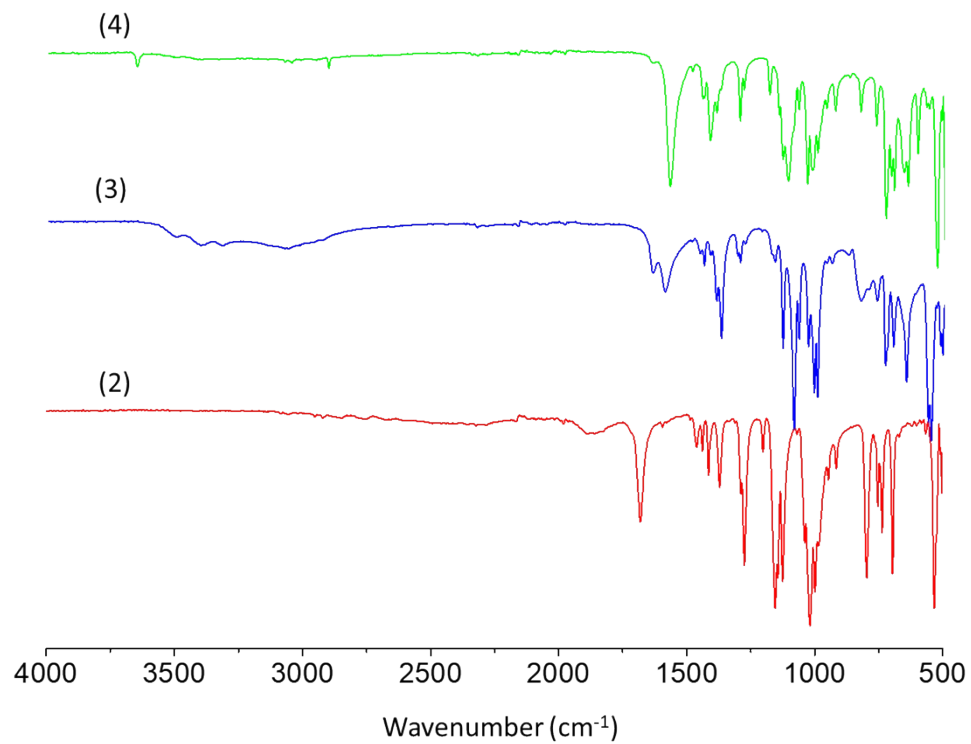


Fig. S4 FT-IR spectra of: (a) $\text{Co}_3(\text{O}_2\text{P}(\text{CH}_2\text{CH}_2\text{COO})(\text{C}_6\text{H}_5))_2(\text{OH})_2$ (4), (b) $\text{Co}_2[(\text{O}_2\text{P}(\text{CH}_2\text{CH}_2\text{COO})(\text{C}_6\text{H}_5)(\text{H}_2\text{O}))_2 \cdot 2\text{H}_2\text{O}$ (3) and (c) $\text{Ca}[\text{O}_2\text{P}(\text{CH}_2\text{CH}_2\text{COO})(\text{C}_6\text{H}_5)]_2$ (2).

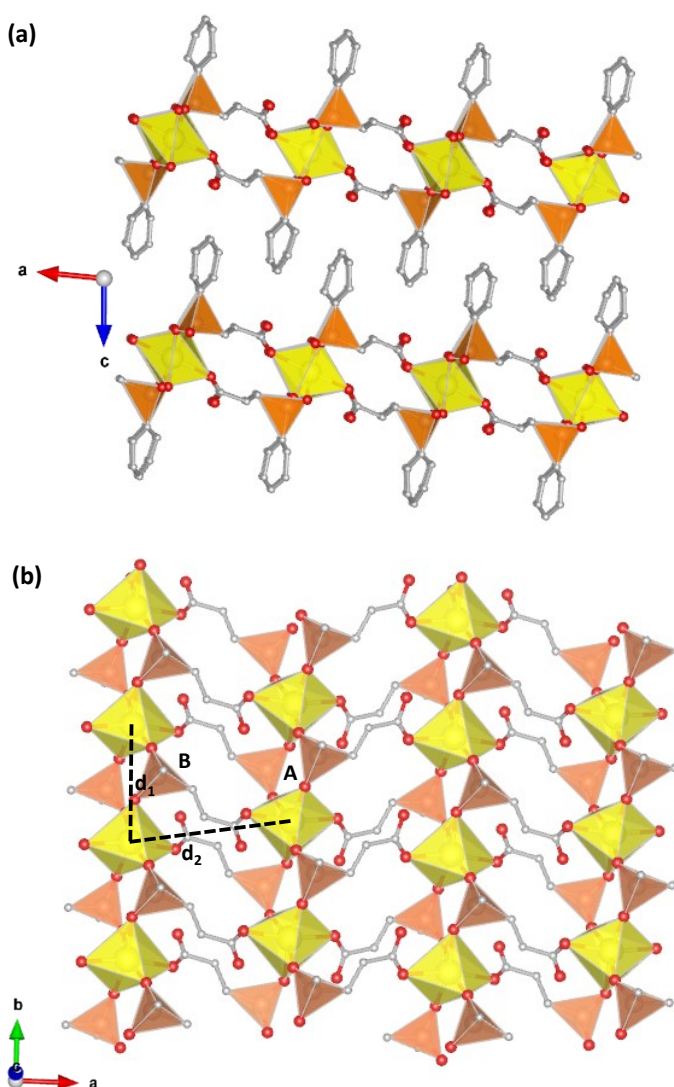


Fig. S5 (a) Layered packing of $\text{Cd}[\text{O}_2\text{P}(\text{CH}_2\text{CH}_2\text{COOH})(\text{C}_6\text{H}_5)]_2$ (**1**) and (b) details of a hybrid layer in $\text{Cd}[\text{O}_2\text{P}(\text{CH}_2\text{CH}_2\text{COOH})(\text{C}_6\text{H}_5)]_2$ (**1**) showing the 8-member rings (A) and 14-member rings (B).

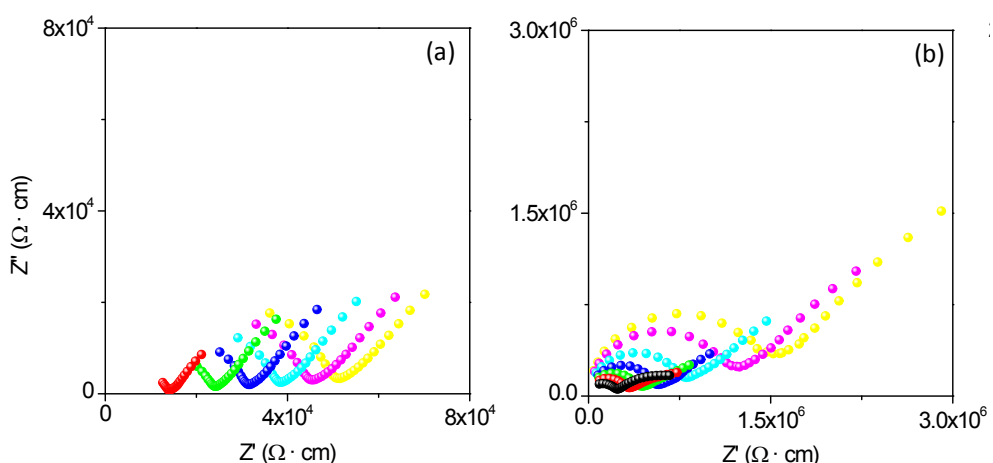


Fig. S6 Plots of the complex impedance plane for (a) **CEPPA ligand** and (b) $\text{Co}_2[(\text{O}_2\text{P}(\text{CH}_2\text{CH}_2\text{COO})(\text{C}_6\text{H}_5)(\text{H}_2\text{O})]_2 \cdot 2\text{H}_2\text{O}$ (**3**) at 95 %RH and various temperatures: 80 (black), 70 (red), 60 (green), 50 (blue), 40 (cyan), 30 (magenta) and 25 °C (yellow).

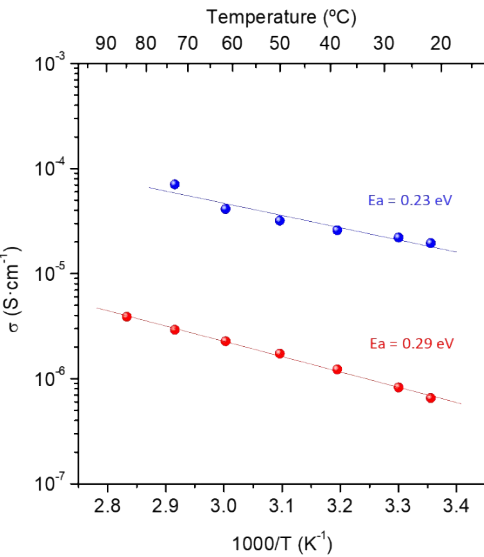


Fig. S7 Arrhenius plots for $\text{Co}_2[(\text{O}_2\text{P}(\text{CH}_2\text{CH}_2\text{COO})(\text{C}_6\text{H}_5)(\text{H}_2\text{O}))_2 \cdot 2\text{H}_2\text{O}$ (**3**) (red) and **CEPPA ligand** (blue) at 95 % RH and different temperatures.

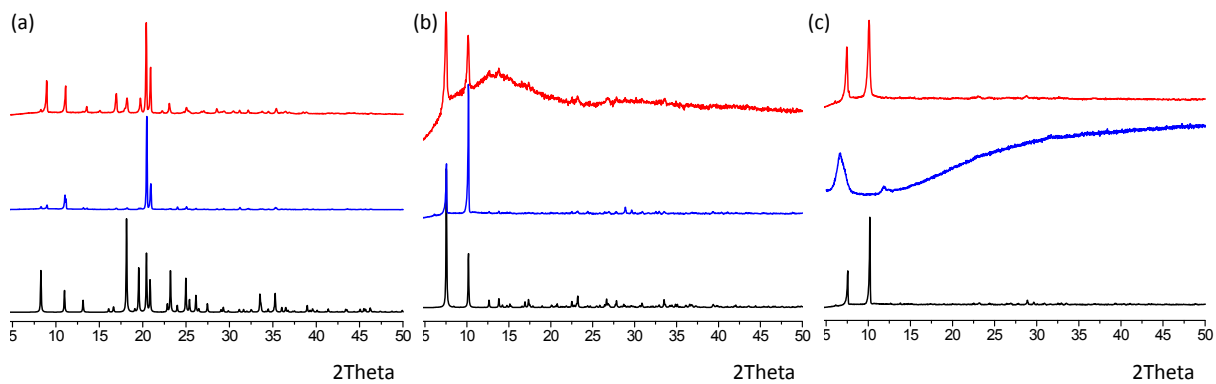


Fig. S8 Comparative of XRPD patterns for (a) **CEPPA** ligand, and (b) $\text{Co}_2[(\text{O}_2\text{P}(\text{CH}_2\text{CH}_2\text{COO})(\text{C}_6\text{H}_5)(\text{H}_2\text{O}))_2 \cdot 2\text{H}_2\text{O}$ (**3**) samples, simulated XRPD (black), as synthetized (blue) and after (red) proton conductivity measurements. (c) XRPD patterns for **3**: as synthetized (black), anhydrous at 200 °C (blue) and rehydrated at 95% RH (red).

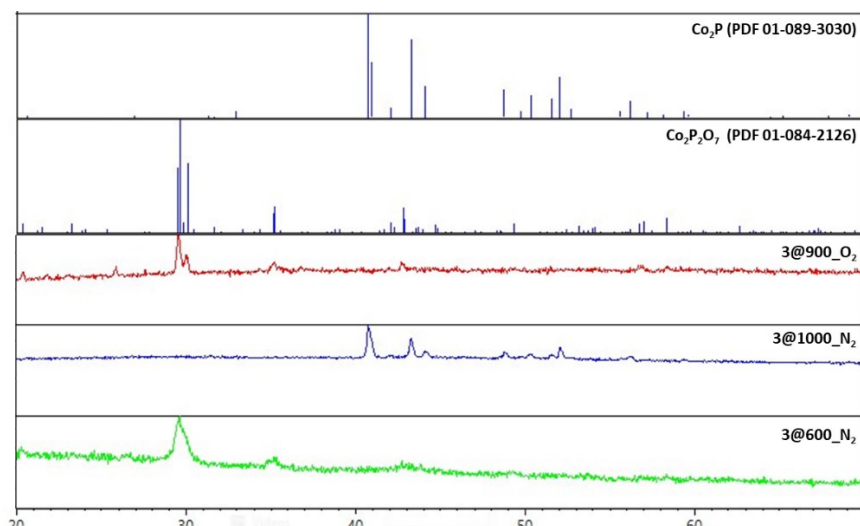


Fig. S9 PXRD patterns of the $\text{Co}_2[(\text{O}_2\text{P}(\text{CH}_2\text{CH}_2\text{COO})(\text{C}_6\text{H}_5)(\text{H}_2\text{O}))_2 \cdot 2\text{H}_2\text{O}$ (**3**) pyrolyzed at different temperatures and atmospheres.

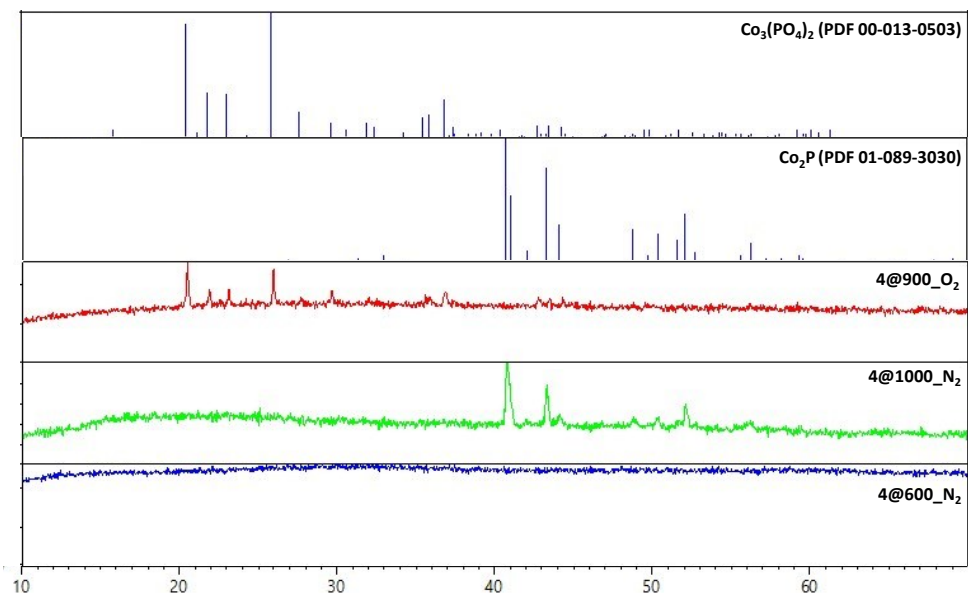


Fig. S10 PXRD patterns of the $\text{Co}_3(\text{O}_2\text{P}(\text{CH}_2\text{CH}_2\text{COO})(\text{C}_6\text{H}_5))_2(\text{OH})_2$ (**4**) pyrolyzed at different temperatures and atmospheres.

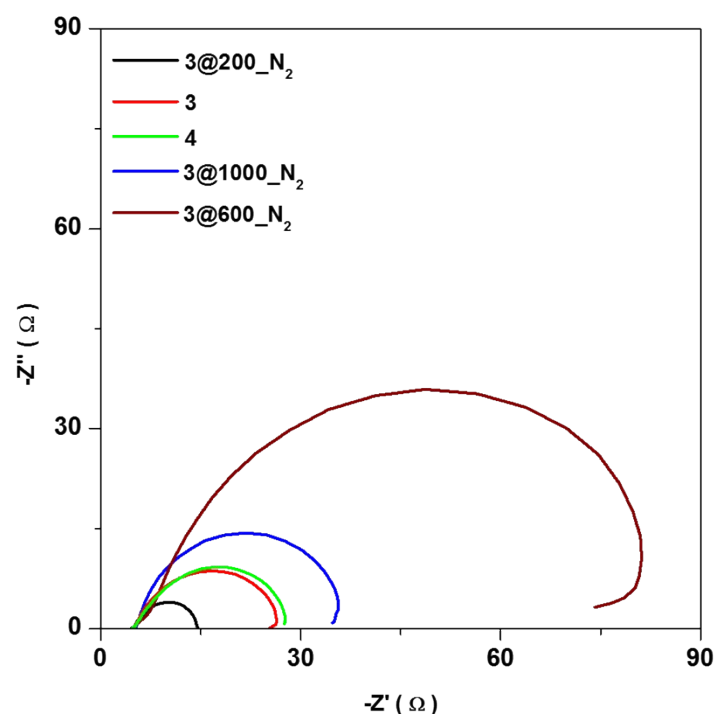


Fig. S11 Nyquist plots for selected cobalt(II) phosphinates and selected calcinated derivatives.

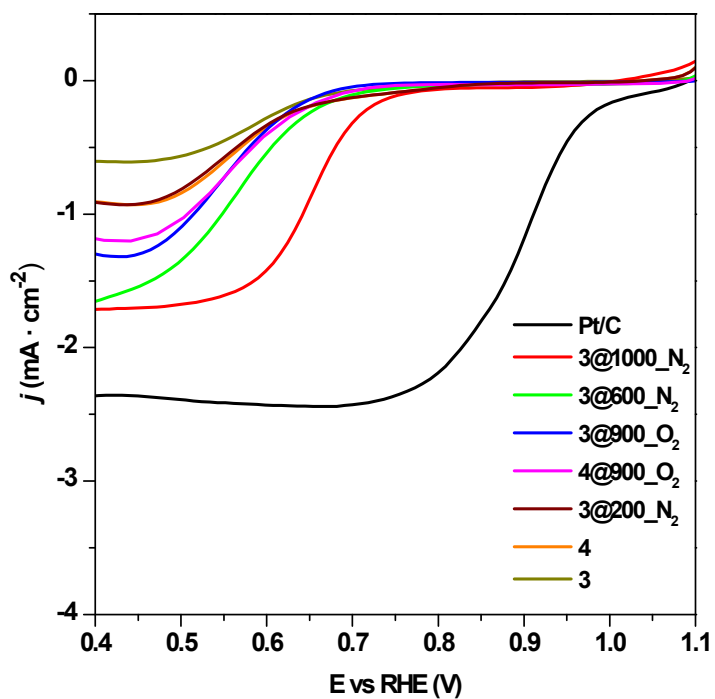


Fig. S12 LSV curves of cobalt(II) phosphinates and their pyrolytic derivatives for the oxygen reduction reaction (ORR).

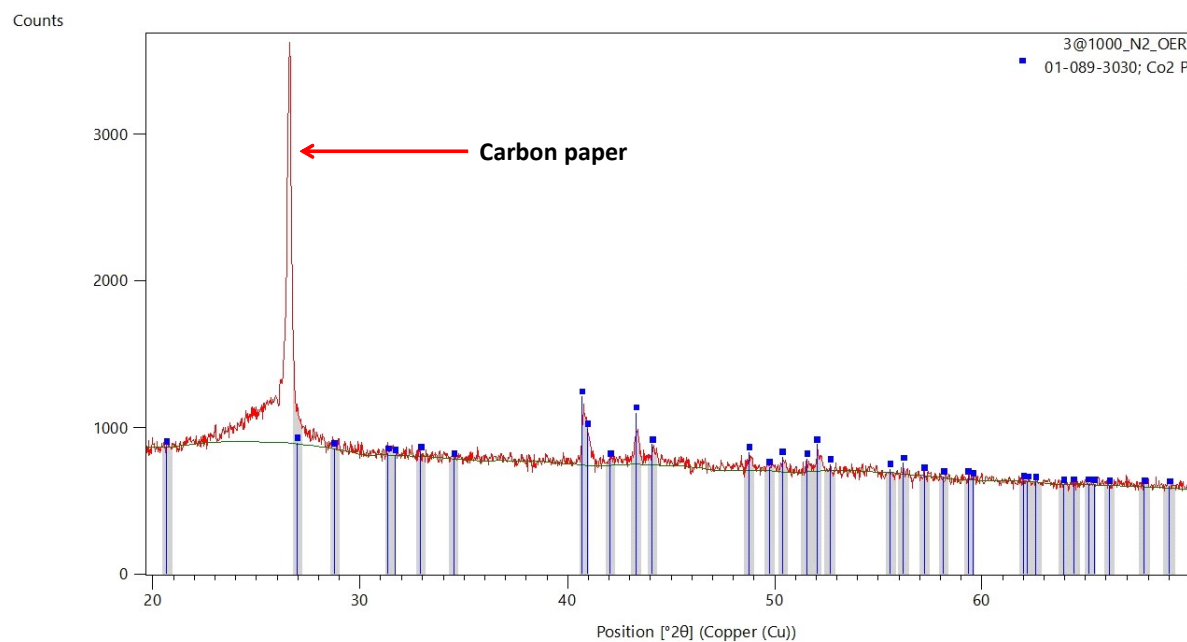


Fig. S13 PXRD pattern of 3@1000C_N₂ after OER test

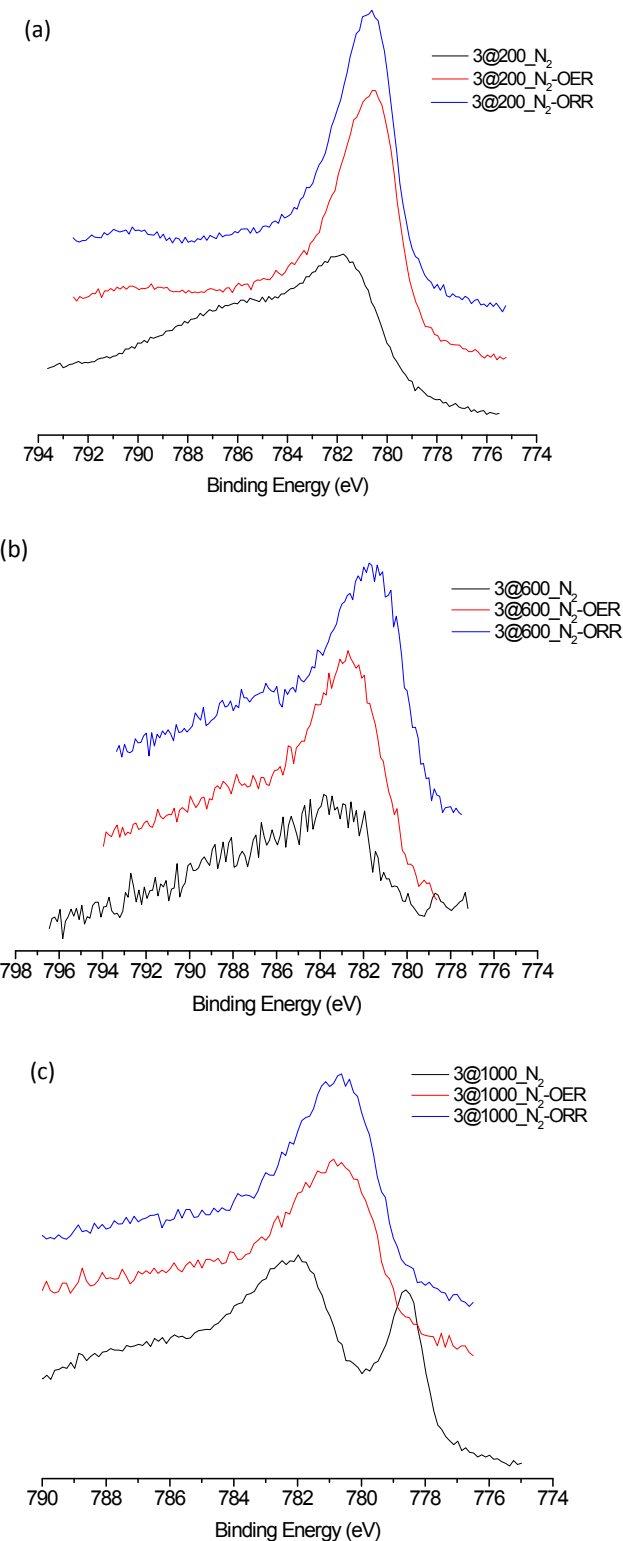


Fig. S14 XPS for Co 2p_{3/2} region of pyrolyzed derivative of compound **3**, before (black line) and after OER (red line) and ORR (blue line) tests.

Table S1. Selected bond lengths (\AA) for compounds **1 – 3**.

Sample	Bond	Length	Bond	Length
1	Cd1 – O1	2.138(12)	P1 – O1	1.530(8)
	Cd1 – O2	2.282(13)	P1 – O2	1.521(8)
	Cd1 – O4	2.336(14)	P1 – C1	1.815(7)
	Cd1 – O5	2.149(12)	P1 – C7	1.811(8)
	Cd1 – O6	2.276(13)		
	Cd1 – O7	2.326(14)		
2	Ca1 – O1	2.573(18)	P1 – O1	1.530(8)
	Ca1 – O2	2.262(14)	P1 – O2	1.529(8)
	Ca1 – O4	2.506(25)	P1 – C1	1.822(7)
	Ca1 – O5	2.286(16)	P1 – C7	1.799(8)
	Ca1 – O6	2.250(14)		
	Ca1 – O7	2.540(24)		
3	Co1 – O11 x 2	2.434(16)	P1 – O11	1.533(11)
	Co1 – O41 x 2	2.270(16)	P1 – O21	1.515(11)
	Co1 – O12 x 2	2.224(16)	P1 – C11	1.836(13)
	Co2 – O21 x 2	2.164(15)	P1 – C41b	1.824(11)
	Co2 – O22 x 2	2.404(15)		
	Co2 – O32 x 2	2.294(16)	P2 – O12	1.580(11)
	Co3 – O11	2.061(15)	P2 – O22	1.513(11)
	Co3 – O41	2.277(17)	P2 – C12	1.805(12)
	Co3 – O22	2.069(15)	P2 – C42b	1.809(11)
	Co3 – O32	2.247(16)		
	Co3 – Ow1	2.025(19)		
	Co3 – Ow2	2.143(16)		

Table S2. H-bond distances for $\text{Co}_2[(\text{O}_2\text{P}(\text{CH}_2\text{CH}_2\text{COO})(\text{C}_6\text{H}_5)(\text{H}_2\text{O})]_2 \cdot 2\text{H}_2\text{O}$ (3).

D-H…A	D…A (\AA)	D-H…A	D…A (\AA)
Ow1…O42	2.613(63)	Ow2…Ow3	2.725(23)
Ow1…Ow4	2.667(23)	Ow3…O21	2.802(24)
Ow1…Ow4	2.682(24)	Ow3…O42	2.715(23)
Ow1…O11	2.948(25)	Ow4…O31	2.751(26)
Ow1…Ow2	2.700(22)	Ow4…O31	2.751(26)
Ow2…O31	2.599(23)	Ow4…O12	2.696(22)

Table S3. XPS data for compound **3** and its pyrolyzed derivatives before and after OER and ORR tests

Sample	B.E. (eV)	Surface Atomic Concentration (%)		
	Co2p _{3/2}	Co	P	Co/P
3	781.37	7.22	5.69	1.27
3-OER	780.01	6.47	0.63	10.27
3-ORR	780.36	8.70	0.38	22.89
3@200_N₂-OER	780.34	4.32	0.39	11.07
3@200_N₂-ORR	780.49	4.13	0.18	22.94
3@600_N₂	781.79	0.74	0.67	1.10
3@600_N₂-OER	781.79	2.51	1.48	1.69
3@600_N₂-ORR	781.16	1.78	0.87	2.04
3@1000_N₂	781.72	5.02	5.85	0.86
3@1000_N₂-OER	780.72	2.27	0.90	2.52
3@1000_N₂-ORR	780.74	1.85	0.63	2.93